

See discussions, stats, and author profiles for this publication at: <https://www.researchgate.net/publication/231373752>

Catalytic Reduction of SO₂ with CO over Supported Iron Catalysts

ARTICLE *in* INDUSTRIAL & ENGINEERING CHEMISTRY RESEARCH · MAY 2006

Impact Factor: 2.59 · DOI: 10.1021/ie0600947

CITATIONS

15

READS

42

6 AUTHORS, INCLUDING:



Ning Li

Chinese Academy of Sciences

60 PUBLICATIONS 969 CITATIONS

SEE PROFILE



Tao Zhang

Fudan University

889 PUBLICATIONS 16,961 CITATIONS

SEE PROFILE

Catalytic Reduction of SO₂ with CO over Supported Iron Catalysts

Xuehai Wang,^{†,‡} Aiqin Wang,[†] Ning Li,[†] Xiaodong Wang,[†] Zhi Liu,^{†,‡} and Tao Zhang^{*,†}

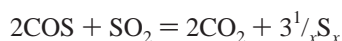
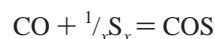
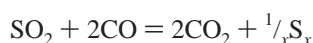
State Key Laboratory of Catalysis, Dalian Institute of Chemical Physics, Chinese Academy of Science, P.O. Box 110, Dalian 116023, China, and Graduate School of the Chinese Academy of Sciences, Beijing, China

Iron oxides supported on several types of carriers (γ -Al₂O₃, HZSM-5, SiO₂, and MgO) were investigated for the catalytic reduction of SO₂ by CO. The catalytic tests show that the activity of the catalysts followed the order Fe₂O₃/ γ -Al₂O₃ > Fe₂O₃/HZSM-5 \gg Fe₂O₃/SiO₂ > Fe₂O₃/MgO. The X-ray diffraction analysis characterization of the presulfided catalysts revealed that FeS₂ formation was greatly dependent on the acidic nature of the supports, with an evident FeS₂ phase detected on both γ -Al₂O₃ and HZSM-5, in contrast with Fe₇S₈ formed on SiO₂ and MgO. Presulfidation with a reacting gas mixture above 500 °C was necessary for obtaining a high activity because of the formation of active-phase FeS₂ during this process. The catalytic activity correlated well with the sulfidation degree of Fe₂O₃, which is mainly dependent on the acidic nature of the support and the choice of the presulfidation conditions. When the Fe content was at 20 wt %, under the optimal feed compositions (CO/SO₂ = 2:1), the Fe₂O₃/ γ -Al₂O₃ catalyst exhibited the best catalytic performance, with 99.31% SO₂ conversion and a 99.17% sulfur yield obtained at 380 °C.

1. Introduction

Sulfur dioxide emitted into the atmosphere as a byproduct of combustion processes, such as coal-fired power plants, is one of the major components of acid rain and other forms of atmospheric pollution.¹ Commercial flue gas desulfurization processes are mostly of the throw-away type in which alkaline materials react with SO₂ to form alkaline metal sulfate that is often stockpiled. Because of the large amount of sulfur dioxide being produced, the disposal of these solid wastes will lead to another environmental problem. To minimize the waste disposal problem associated with the existing technologies, several regenerable sulfur dioxide scrubbing systems have been developed.² In these regeneration processes, sulfur dioxide from flue gas is first absorbed in an alkaline solution or adsorbed on a solid substrate and is subsequently desorbed to produce a stream of high-concentration sulfur dioxide. The recovery of elemental sulfur from this stream in a single-stage catalytic converter would be the best choice for it is easy to treat, handle, and transport and there are no secondary pollution issues.^{3,4}

Direct reduction of sulfur dioxide by carbon monoxide is a promising approach for the recovery of elemental sulfur because CO is converted to CO₂ and simultaneously removed from the flue gas stream.^{5,6} The overall reactions involved in this process are as follows:



where $x = 2$ –8 or higher. A part of S_x can further react with CO to form carbonyl sulfide, COS. This, in turn, may again

reduce SO₂ to elemental sulfur. However, COS is a more toxic compound than SO₂, and its production should be minimized in a sulfur recovery process.

So far, the catalytic reduction of SO₂ to elemental sulfur with CO as reducing agent has been extensively studied using various types of catalysts including perovskite,^{7–10} mixed oxides,^{11–15} and alumina-supported transition metals.^{16–21} Both perovskite and mixed oxides required a high reaction temperature (above 500 °C) to obtain complete conversion of SO₂, although they possessed the advantage of high selectivity to sulfur formation (COS formation was largely limited).^{9,11} To lower the light-off temperature, Chen and Weng¹⁴ employed nanosized CeO₂ as a support and found that Cr₂O₃/nano-CeO₂ exhibited the highest activity with full SO₂ conversion at 320 °C. However, compared with other widely used commercial supports, such as alumina and silica, the high cost of nano-CeO₂ limits its application to some extent.

On the other hand, alumina-supported transition metals were the earliest-studied catalysts for SO₂ reduction with CO. However, in the early development of the alumina-supported catalyst, a substantial amount of COS, which is much more harmful than SO₂, was formed as a byproduct during the SO₂ reduction by CO.^{16–18,21} This is probably because the alumina support used in their work was α -Al₂O₃ and the preparation method was simple mechanical mixing. Instead, using γ -Al₂O₃ as the support, Lee and Han found that about a 97% conversion of sulfur dioxide and selectivity to elemental sulfur were achieved at temperatures above 400 °C over LaNi/ γ -Al₂O₃.²⁰ Recently, Zhuang et al. found that CoMo/Al₂O₃, which had been used primarily for hydrodesulfurization reactions, exhibited very high activity and selectivity for the reduction of sulfur dioxide by CO,¹⁹ with a complete conversion of SO₂ at 300 °C. This is one of the most active catalysts reported so far for SO₂ reduction with CO, showing the great potential of alumina-supported transition metals as catalysts for this reaction.

A careful comparison of the catalytic activities of alumina-supported transition metals in the literature reveals that the textural properties of alumina have an important effect on the catalytic performance of the metals supported on it. Prompted

* To whom correspondence should be addressed. Tel.: +86-411-84379015. Fax: +86-411-84691570. E-mail: taozhang@dicp.ac.cn.

[†] Chinese Academy of Science.

[‡] Graduate School of the Chinese Academy of Sciences.

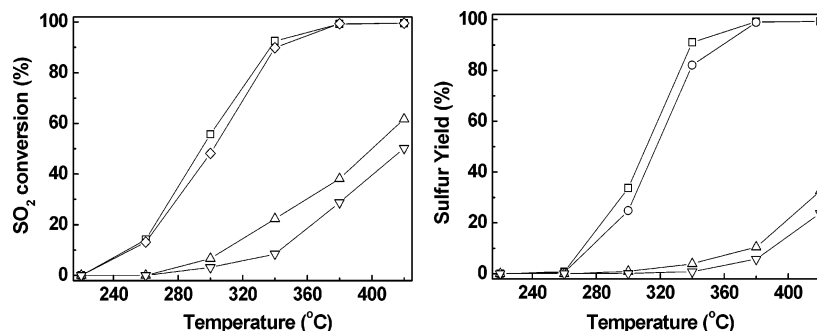


Figure 1. Effect of support nature on SO_2 conversion and sulfur yield. (\square) $\text{Fe}_2\text{O}_3/\gamma\text{-Al}_2\text{O}_3$, (\diamond) $\text{Fe}_2\text{O}_3/\text{HZSM-5}$, (\triangle) $\text{Fe}_2\text{O}_3/\text{SiO}_2$, and (∇) $\text{Fe}_2\text{O}_3/\text{MgO}$. Feed compositions: 5000 ppm SO_2 and 10 000 ppm CO, SV = 18 000 mL/g h.

by this, we believe that $\text{Fe}/\text{Al}_2\text{O}_3$, which was initially investigated by Khalafalla et al.^{16,17,21} for the catalytic reduction of SO_2 by CO, may be undervalued, because the low surface area of $\alpha\text{-Al}_2\text{O}_3$ would make the active phase poorly dispersed. In this paper, we used $\gamma\text{-Al}_2\text{O}_3$, ZSM-5, silica, and MgO to support Fe_2O_3 and found that the $\text{Fe}_2\text{O}_3/\gamma\text{-Al}_2\text{O}_3$ catalyst exhibited the highest catalytic activity, with 99.31% SO_2 conversion at around 380 °C. More importantly, the formation of COS was largely limited, and the COS concentration was less than 60 ppm above 380 °C.

2. Experimental Section

2.1. Catalyst Preparation. $\gamma\text{-Al}_2\text{O}_3$ (homemade, surface area 238 m^2/g , pore volume 0.35 cm^3/g), HZSM-5 ($\text{SiO}_2/\text{Al}_2\text{O}_3 = 25$, surface area 365 m^2/g , supplied by NanKai University, China), SiO_2 (surface area 400 m^2/g , Qingdao Ocean Chemical Company, China), and MgO (surface area 35 m^2/g , AR grade, Shenyang Agent Company, China) were used as catalyst supports. The supports were impregnated with an appropriate aqueous solution of $\text{Fe}(\text{NO}_3)_3 \cdot 9\text{H}_2\text{O}$. Then, the samples were dried at 120 °C for 12 h and calcined at 500 °C for 5 h. In the tests for the influence of Fe content, the loading of Fe that was calculated on an Fe_2O_3 basis was varied between 2.5 and 40 wt %, while Fe loading was fixed at 20 wt % for other tests. All of the catalysts were pelletized, crushed, and sieved to 40–60 mesh for use in activity tests.

2.2. Activity Measurement. The catalytic reaction between SO_2 and CO was carried out in a fixed-bed flow reactor system at atmospheric pressure. A total of 0.2 g of the catalyst was placed in a quartz reactor (6 mm i.d.). After being purged in a He flow (36 mL/min) at 500 °C for 2 h, the catalyst was in situ presulfided with a reaction gas mixture containing 10 000 ppm CO and 5000 ppm SO_2 in He at a flow rate of 60 mL/min at 500 °C for 2 h. In some cases, a different presulfidation temperature (400, 500, or 600 °C) was employed in order to compare the effects of presulfidation methods. After presulfidation, the catalyst was cooled to 220 °C for activity tests. The feed gas typically consisted of 10 000 ppm CO and 5000 ppm SO_2 except for testing the effect of feed concentration. The effluent gas was passed through an ice-water trap, where elemental sulfur was condensed. Concentrations of SO_2 and COS in the effluent gas were separated by a Gaspro capillary column and detected by a flame photometric detector, while CO and CO_2 were separated by a Porapak Q column and detected by a thermal conductivity detector (TCD).

The percent conversion (X) of SO_2 and the selectivity (S) and percent yield (Y_s) of elemental sulfur are defined as follows:

$$X = \frac{[\text{SO}_2]_{\text{in}} - [\text{SO}_2]_{\text{out}}}{[\text{SO}_2]_{\text{in}}} \times 100\%$$

$$S = \frac{[\text{SO}_2]_{\text{in}} - [\text{SO}_2]_{\text{out}} - [\text{COS}]_{\text{out}}}{[\text{SO}_2]_{\text{in}} - [\text{SO}_2]_{\text{out}}} \times 100\%$$

$$Y_s = XS$$

where $[\text{SO}_2]_{\text{in}}$ is the inlet concentration of SO_2 and $[\text{SO}_2]_{\text{out}}$ and $[\text{COS}]_{\text{out}}$ are the outlet concentrations of SO_2 and COS, respectively.

2.3. NH_3 Temperature-Programmed Desorption (NH_3 -TPD) and CO_2 -TPD Measurements. NH_3 -TPD of the three acidic supports (HZSM-5, $\gamma\text{-Al}_2\text{O}_3$, and SiO_2) and CO_2 -TPD of the MgO support were measured with the Micromeritics AutoChem II 2920 Automated Catalyst Characterization System. A total of 150 mg of the sample was placed in a quartz reactor. Before each experiment, the sample was treated in a He flow at 600 °C for 30 min at a flow rate of 30 mL/min in order to remove water and other contaminants. Then, the reactor was cooled to 100 °C for NH_3 adsorption or 50 °C for CO_2 adsorption. After the saturation of adsorption of NH_3 (or CO_2) was reached at that temperature, the reactor was heated from 100 °C (or 50 °C for CO_2) to 600 °C at a rate of 10 °C/min, and the NH_3 -TPD (or CO_2 -TPD) spectra were recorded with a TCD as a detector.

2.4. CO Temperature-Programmed Reduction (CO-TPR) Measurement. CO-TPR of the $\text{Fe}_2\text{O}_3/\gamma\text{-Al}_2\text{O}_3$ was performed using the same system as that described for $\text{NH}_3(\text{CO}_2)$ -TPD. A total of 150 mg of the sample was placed in a quartz reactor. Before each experiment, the sample was treated in a He flow at 100 °C for 30 min at a flow rate of 30 mL/min in order to remove physically adsorbed water. Then, the reactor was cooled to room temperature and heated to 700 °C at a rate of 10 °C/min. The CO-TPR spectra were recorded with a mass spectrometer as a detector.

2.5. X-ray Diffraction Analysis (XRD) Measurements. XRD patterns were obtained with a Rigaku (D/MAX- β B) diffractometer equipped with an online computer. Ni-filtered $\text{Cu K}\alpha$ radiation was used.

3. Results and Discussion

3.1. The Effect of Support Natures. In this study, we chose four types of material as the catalyst supports, including $\gamma\text{-Al}_2\text{O}_3$, HZSM-5, SiO_2 , and MgO. These four supports are widely used in the chemical industry and with different acid–base natures. The SO_2 conversion and sulfur yield on these four different supported Fe_2O_3 catalysts are illustrated in Figure 1. Both the

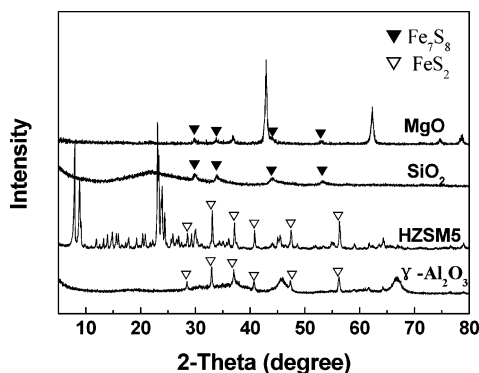
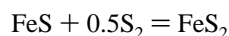
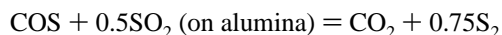
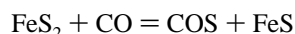


Figure 2. X-ray diffraction patterns of four different supported Fe_2O_3 catalysts after sulfidation at 500 °C for 2h.

SO_2 conversion and the sulfur yield follow the order $\text{Fe}_2\text{O}_3/\gamma\text{-Al}_2\text{O}_3 > \text{Fe}_2\text{O}_3/\text{HZSM-5} \gg \text{Fe}_2\text{O}_3/\text{SiO}_2 > \text{Fe}_2\text{O}_3/\text{MgO}$. Especially, when $\gamma\text{-Al}_2\text{O}_3$ and HZSM-5 were used as the support, the catalysts were very active and selective. A total of 99.31% SO_2 conversion and 99.17% sulfur yield were obtained over $\text{Fe}_2\text{O}_3/\gamma\text{-Al}_2\text{O}_3$ at a reaction temperature of 380 °C. Meanwhile, the COS concentration in the effluent gas was lower than 60 ppm. In contrast, the SO_2 conversion and sulfur yield were lower than 40% over SiO_2 - and MgO-supported catalysts at 380 °C.

Khallafalla^{16,17} et al. proposed the following carbonyl sulfide intermediate mechanism when they investigated SO_2 reduction with CO over $\text{Fe}/\text{Al}_2\text{O}_3$:



According to this mechanism, FeS_2 was the active phase for the catalytic reduction of SO_2 . To examine the effect of support nature on FeS_2 formation, we conducted an XRD detection on the four catalysts after sulfidation, as shown in Figure 2. On the sulfided $\text{Fe}_2\text{O}_3/\gamma\text{-Al}_2\text{O}_3$ and $\text{Fe}_2\text{O}_3/\text{HZSM-5}$ catalysts, the diffraction peaks corresponding to FeS_2 ($2\theta = 28.5^\circ, 33.0^\circ, 37.1^\circ, 40.8^\circ, 47.4^\circ$, and 56.3°) were clearly observed, indicating that an FeS_2 crystalline phase was formed during sulfidation. In contrast, the XRD patterns of sulfided $\text{Fe}_2\text{O}_3/\text{SiO}_2$ and $\text{Fe}_2\text{O}_3/\text{MgO}$ show four peaks at 2θ of around $30.0^\circ, 34.0^\circ, 44.0^\circ$, and 53.3° , characteristic of pyrrhotite (specifically, Fe_7S_8), indicating that the sulfidation of $\text{Fe}_2\text{O}_3/\text{SiO}_2$ and $\text{Fe}_2\text{O}_3/\text{MgO}$ was not sufficient. Because iron disulfide is a relatively unstable sulfide and can be more easily reduced by CO to form the intermediate COS,²⁰ FeS_2 is generally thought of as an active phase for SO_2 reduction with CO. Therefore, we can conclude from the above XRD characterizations that variation of the support will lead to a great difference in the degree of sulfidation and thereby affects the catalytic activity for SO_2 reduction with CO.

The four supports employed in this work differ mainly in their acid–base properties. To give quantitative evidence, we conducted NH_3 -TPD experiments on the $\gamma\text{-Al}_2\text{O}_3$, HZSM-5, and SiO_2 supports and CO_2 -TPD experiments on the MgO support to determine their acid–base properties. The TPD curves are shown in Figure 3. These results are consistent with those reported in the literature.^{22–25} In the TPD profiles, the number of the acidic/basic sites is reflected in the peak area, and the strength of the acidic/basic sites is reflected by the maximum desorption temperature. For HZSM-5, two peaks can be

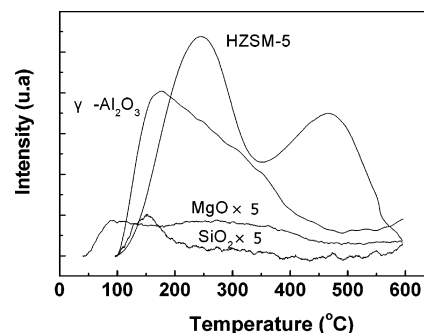


Figure 3. NH_3 -TPD spectra of $\gamma\text{-Al}_2\text{O}_3$, HZSM-5, and SiO_2 and CO_2 -TPD spectrum of MgO.

Table 1. Comparison of SO_2 Conversions over the Four Supports and the Four Catalysts^a

supports	SO_2 conversion	catalysts	SO_2 conversion
$\gamma\text{-Al}_2\text{O}_3$	76.43	$\text{Fe}_2\text{O}_3/\gamma\text{-Al}_2\text{O}_3$	64.33
HZSM-5	74.36	$\text{Fe}_2\text{O}_3/\text{HZSM-5}$	62.38
SiO_2	18.63	$\text{Fe}_2\text{O}_3/\text{SiO}_2$	12.47
MgO	10.11	$\text{Fe}_2\text{O}_3/\text{MgO}$	8.58

^a Feed compositions: 5000 ppm SO_2 and 10 000 ppm COS, SV = 18 000 mL/g h. Reaction temperature: 300 °C.

distinguished: one at 245 °C can be attributed to the weak acid sites, and the other at about 470 °C belongs to the strong acid sites. The NH_3 -TPD spectrum of $\gamma\text{-Al}_2\text{O}_3$ contains a very broad signal from 100 to 500 °C, which can be ascribed to the NH_3 desorbed from the acid sites with low and medium to high strength, while for SiO_2 , a very weak ammonia desorption peak was found at 150 °C. Clearly, from the NH_3 -TPD, we can see that both the acid strengths and the acid numbers of the three supports follow the order HZSM-5 > $\gamma\text{-Al}_2\text{O}_3 \gg \text{SiO}_2$. On the other hand, the MgO support does not adsorb NH_3 at all, but it can adsorb a small amount of CO_2 , which is indicated by a very weak and broad CO_2 desorption peak at temperatures ranging from 50 to 450 °C, showing the weakly basic nature of MgO. Thus, the acidity of the four supports follows the order HZSM-5 > $\gamma\text{-Al}_2\text{O}_3 \gg \text{SiO}_2 > \text{MgO}$. This order coincides very well with the degree of sulfidation. Therefore, we can conclude that acidic support will facilitate the formation of FeS_2 . On the other hand, we also found that acidic support can speed up the reaction between COS and SO_2 , as shown in Table 1. It was suggested that, in the case of acidic support, the carbonyl sulfide chemisorbed cationically on the Lewis acid sites and the sulfur dioxide chemisorbed anionically on the Brønsted sites, allowing the adsorbed species to react according to a Langmuir–Hinshelwood mechanism.¹⁷ Acid sites will facilitate them to adsorb and react with each other. Therefore, in our catalyst systems, acid supports had dual functions: one is to facilitate the formation of active-phase FeS_2 ; the other is to speed up the reaction between COS and SO_2 . Finally, we should mention that the minor discrepancy between the activity level and the acidity of $\text{Fe}_2\text{O}_3/\text{HZSM-5}$ may be due to the diffusion limits of the micropores of the HZSM-5 support.

3.2. The Effect of Sulfidation Methods. From the above XRD results, we know that Fe_2O_3 is transformed to active species FeS_2 in the process of presulfidation. Therefore, sulfidation is the key step to activating the catalyst for SO_2 reduction with CO. In this work, we investigated in detail the effect of the sulfidation temperature on the catalytic behavior of $\text{Fe}_2\text{O}_3/\gamma\text{-Al}_2\text{O}_3$, and the results are shown in Figure 4. We can see that the catalysts presulfided above 500 °C have a similar activity, whereas the catalysts presulfided at 400 °C show a lower activity. In addition, presulfidation under a temperature-

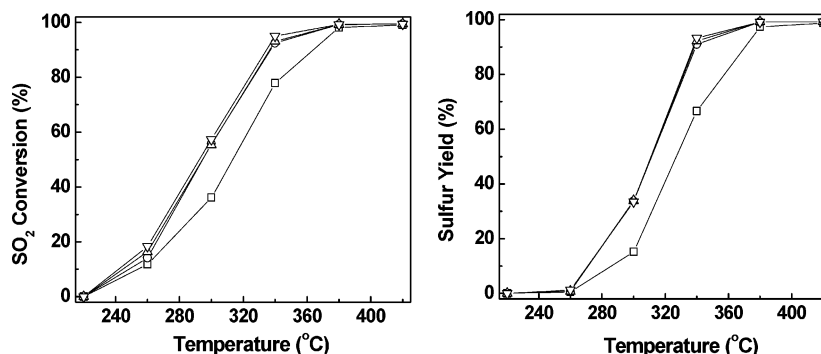


Figure 4. SO₂ conversion and sulfur yield over Fe₂O₃/γ-Al₂O₃ presulfided at (□) 400 °C, (◇) 500 °C, and (Δ) 600 °C and (▽) by temperature-programmed mode. Feed compositions: 5000 ppm SO₂ and 10 000 ppm CO, SV = 18 000 mL/g h.

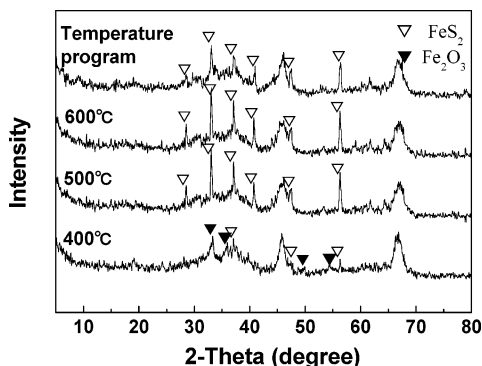


Figure 5. X-ray diffraction patterns of Fe₂O₃/γ-Al₂O₃ under different sulfidation conditions.

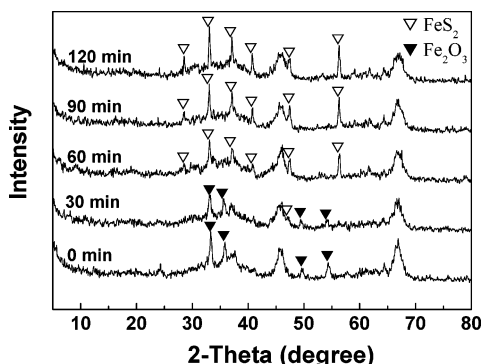


Figure 6. X-ray diffraction patterns of Fe₂O₃/γ-Al₂O₃ under different sulfidation times.

programmed mode (the temperature was first increased from 300 to 500 °C over 200 min, then kept at 500 °C for 30 min) seems to have no effect on the catalytic performance, as long as the sulfidation temperature was above 500 °C.

The XRD patterns of Fe₂O₃/γ-Al₂O₃ after sulfidation at different temperatures are depicted in Figure 5. FeS₂ was the only Fe species when sulfidation occurred above 500 °C, while both Fe₂O₃ ($2\theta = 33.2^\circ$, 49.5° , and 54.1°) and FeS₂ were observed when sulfidation occurred at 400 °C. Clearly, 400 °C is not high enough to completely presulfide Fe₂O₃ to FeS₂. Full sulfidation was obtained at temperatures above 500 °C, and temperature-programmed sulfidation does not improve the activity of the catalyst.

To further investigate how the phase transformation from Fe₂O₃ to FeS₂ occurred during the sulfidation process, Fe₂O₃/γ-Al₂O₃ was subjected to an X-ray diffraction analysis after a certain period of sulfidation at 500 °C, and the corresponding XRD peaks are depicted in Figure 6. It can be seen that Fe₂O₃ was the only Fe phase on the catalyst before sulfidation. After

sulfidation for 30 min, the XRD peak intensity of Fe₂O₃ decreased and FeS₂ ($2\theta = 47.4^\circ$) appeared. When sulfidation proceeded for 60 min, no Fe₂O₃ phase was detected. With the sulfidation time further prolonged, the intensity of FeS₂ became even stronger. This result indicates that the phase transformation from Fe₂O₃ to FeS₂ will not be complete until sulfidation has occurred at 500 °C for 2 h.

To reveal the sulfidation mechanism of Fe₂O₃/γ-Al₂O₃ with a reacting gas mixture, we detected the changes in the effluent gas concentration with time when the catalyst was pretreated by SO₂, CO, or a mixture of the two gases. Figure 7 presents the results. When only 5000 ppm SO₂ passed over the catalyst (Figure 7a), the effluent concentration of SO₂ first decreased to zero at 10 min and then increased quickly to its initial value. The decline of SO₂ concentration at the initial 10 min was probably due to SO₂ adsorption on Fe₂O₃/γ-Al₂O₃. When only 10 000 ppm CO passed over the catalyst (Figure 7b), the effluent CO gas concentration change was very similar to the case of SO₂; meanwhile, the formation of CO₂ was observed in line with the CO consumption, indicating that CO was oxidized by Fe₂O₃ to form CO₂ in the initial stage. In contrast, when 5000 ppm SO₂ and 10 000 ppm CO simultaneously passed over the catalyst, the SO₂ concentration first decreased to zero at 10 min and then increased quickly to a maximum of 2580 ppm (about half of the initial concentration) at 30 min. After that, the SO₂ concentration decreased gradually to zero. The CO concentration decreased more sharply during the initial 10 min, then leveled at a low value as the sulfidation progressed. In contrast, the CO₂ concentration increased quickly at the initial stage and then leveled at a high value. To confirm that the CO consumption was due to the reduction of Fe₂O₃, a TPR of Fe₂O₃/γ-Al₂O₃ with CO as the reductant was conducted, and the results are shown in Figure 8. Three reduction peaks were observed. The two peaks positioned at 327 and 370 °C can be attributed to the reduction of Fe₂O₃ to Fe₃O₄ and of Fe₃O₄ to FeO, respectively, and the third peak positioned at 620 °C is due to the reduction of FeO to Fe.^{26,27} However, XRD detection of the CO-reduced samples at 500 and 700 °C reveals the formation of Fe₃O₄ at 500 °C and Fe at 700 °C (Figure 9). We did not detect the existence of FeO or Fe at 500 °C probably because they were low in amount below the XRD detection limits or because they were reoxidized by air when subjected to XRD examination. On the basis of the above experimental results, though a detailed sulfidation mechanism is not clear with CO and SO₂, it is speculated as follows. In the initial stage, most of the CO was consumed by Fe₂O₃ and reduced Fe₂O₃ to Fe₃O₄, FeO, and Fe, while another smaller amount of CO was able to reduce SO₂ to sulfur; sulfur then reacted with the reduced Fe species to form FeS₂. Once FeS₂ was produced, the catalytic reaction between SO₂ and CO on FeS₂ was very fast.

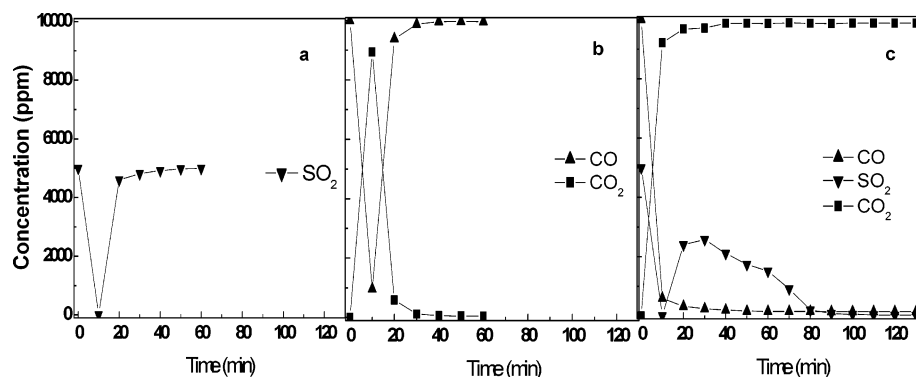


Figure 7. Changes in effluent gas concentration with reaction time under different feed compositions at 500 °C over $\text{Fe}_2\text{O}_3/\gamma\text{-Al}_2\text{O}_3$. Feed gas compositions: (a) 5000 ppm SO_2 , (b) 10 000 ppm CO, and (c) 5000 ppm SO_2 and 10 000 ppm CO.

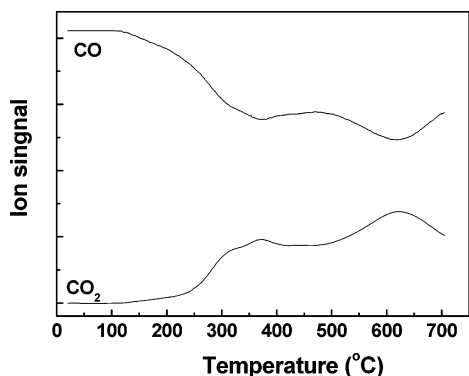


Figure 8. CO-TPR profile of $\text{Fe}_2\text{O}_3/\gamma\text{-Al}_2\text{O}_3$.

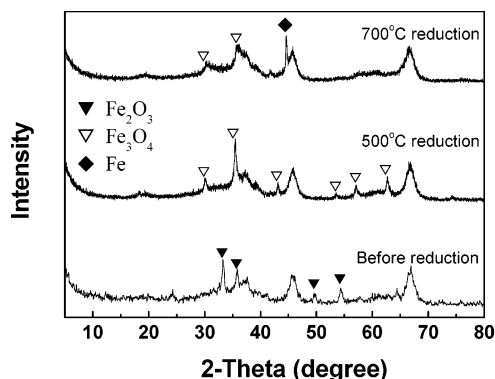


Figure 9. X-ray diffraction patterns of $\text{Fe}_2\text{O}_3/\gamma\text{-Al}_2\text{O}_3$ before reduction, after 500 °C reduction, and after 700 °C reduction.

3.3. The Effect of Fe Content. From the above results, it can be found that $\text{Fe}_2\text{O}_3/\gamma\text{-Al}_2\text{O}_3$ and $\text{Fe}_2\text{O}_3/\text{HZSM-5}$ exhibited similar activities and selectivities. However, from the perspective of industrial application, $\text{Fe}_2\text{O}_3/\gamma\text{-Al}_2\text{O}_3$ is more promising than $\text{Fe}_2\text{O}_3/\text{HZSM-5}$ because of the higher hydrothermal stability and mechanical strength of $\gamma\text{-Al}_2\text{O}_3$. Therefore, further study on the optimization of parameters was focused on for $\text{Fe}_2\text{O}_3/\gamma\text{-Al}_2\text{O}_3$. First of all, the effect of Fe content in $\text{Fe}_2\text{O}_3/\gamma\text{-Al}_2\text{O}_3$ on catalytic performance was investigated, and the results are shown in Figure 10. We noted that there was no reaction between SO_2 and CO occurring with $\gamma\text{-Al}_2\text{O}_3$ as a catalyst in the temperature range investigated. In fact, substantial SO_2 conversion over $\gamma\text{-Al}_2\text{O}_3$ was not observed until 600 °C. This is in agreement with that reported by Lee and Han.²⁰ However, with an increase of Fe content from 0 to 20%, both the SO_2 conversion and the sulfur yield increased and reached their maxima at an Fe content of 20%. Then, with a further increase of Fe content, the conversion and sulfur yield decreased. Hence, 20% is the optimum content of Fe on the $\gamma\text{-Al}_2\text{O}_3$ support, at which the

synergistic effect between the Fe species and $\gamma\text{-Al}_2\text{O}_3$ would act best to catalytically reduce SO_2 with CO. Excess Fe content (beyond 20 wt %) will probably lead to a decreased dispersion degree of the active phase (FeS_2). When the Fe content was 20%, a 92.5% SO_2 conversion and a 91.8% sulfur yield were obtained at 340 °C over $\text{Fe}_2\text{O}_3/\gamma\text{-Al}_2\text{O}_3$.

3.4. The Effect of Feed Gas Composition. To obtain the optimal operating conditions, we investigated the effect of different feed ratios of CO/ SO_2 on the efficiency of SO_2 reduction. Because the complete reduction of 1 mole of SO_2 needs 2 moles of CO ($2\text{CO} + \text{SO}_2 = 2\text{CO}_2 + \text{S}$), the feed ratio of CO/ SO_2 was varied from 1:1 to 3:1, while the SO_2 concentration was fixed at 5000 ppm. From Figure 11, we can see that, when the feed ratio of CO/ SO_2 is 1:1, that is, CO is insufficient, SO_2 conversion and the sulfur yield are less than 50%. When the feed ratio of CO/ SO_2 is 3:1, that is, CO is in excess, SO_2 conversion is the highest while the sulfur yield is at the lowest below 400 °C because of a substantial amount of COS formed via the reaction between CO and S. Similar results were also observed by Zhuang et al.¹⁹ and Chen and Weng.¹⁴ Excess CO reacted with elemental sulfur to produce COS at low temperatures, while COS is unstable and decomposed into CO and S at higher temperatures. Therefore, the sulfur yield increased with the temperature. When CO/ SO_2 is at a stoichiometric molar ratio of 2:1, the highest SO_2 conversion and sulfur yield can be obtained.

Knowing that the optimal ratio of CO/ SO_2 is 2:1 and that the feed concentrations of CO and SO_2 may affect the efficiency of SO_2 reduction, four different feed concentrations (CO/ SO_2 = 5000:2500, 10 000:5000, 15 000:7500, and 20 000:10 000, all in ppm) were employed to assess their influence. Figure 12 manifests that low feed concentrations of CO and SO_2 provide a higher reduction rate of SO_2 and a higher yield of elemental sulfur. SO_2 conversions under four different feed concentrations were 94.5%, 92.5%, 86.1%, and 79.3% at 340 °C, respectively. However, at a temperature of 380 °C, a high SO_2 conversion and sulfur yield (COS concentration in effluent gas was lower than 90 ppm) were all obtained whatever SO_2 inlet concentration was used.

Considering that O_2 , H_2O , and CO_2 are often present in the flue gas, there is a necessity to investigate the effect of O_2 , H_2O , or CO_2 on the performance of the catalysts. As shown in Figure 13, when the feed gas contained 0.5% oxygen, both the SO_2 conversion and the sulfur yield decreased sharply. The SO_2 conversion dropped down to 29.41% after 60 min of reaction time. An XRD analysis of the used catalyst revealed that FeS_2 had been transformed to Fe_2O_3 . After the removal of O_2 , the catalytic activity restored slowly. When the feed gas contained 4% water vapor, the SO_2 conversion decreased gradually from

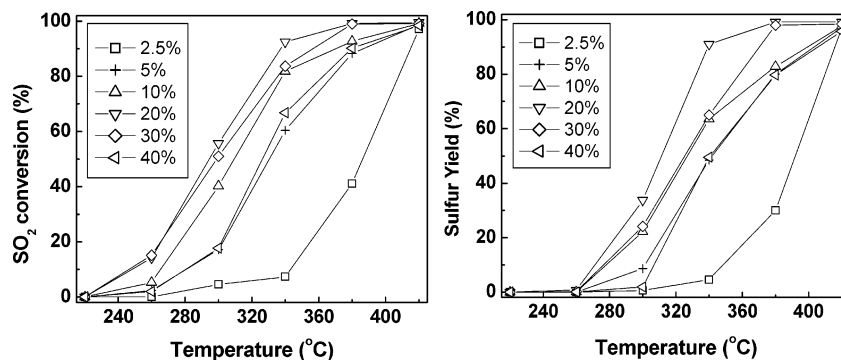


Figure 10. Effect of Fe content in $\text{Fe}_2\text{O}_3/\gamma\text{-Al}_2\text{O}_3$ on SO_2 conversion and sulfur yield. Feed compositions: 5000 ppm SO_2 and 10 000 ppm CO, SV = 18 000 mL/g h.

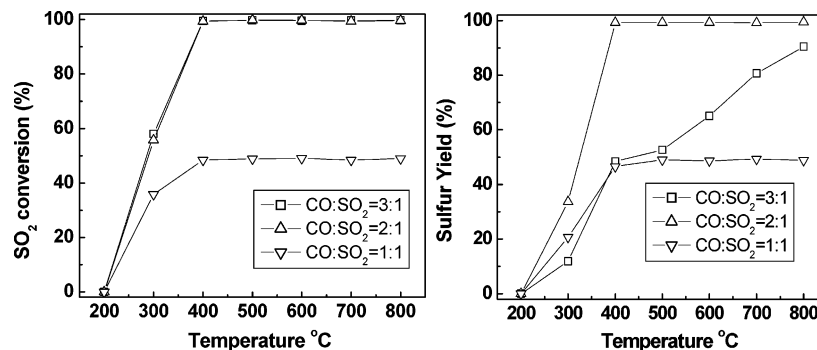


Figure 11. Effect of molar ratios of CO/ SO_2 on SO_2 conversion and sulfur yield over $\text{Fe}_2\text{O}_3/\gamma\text{-Al}_2\text{O}_3$ (SV = 18 000 mL/g h).

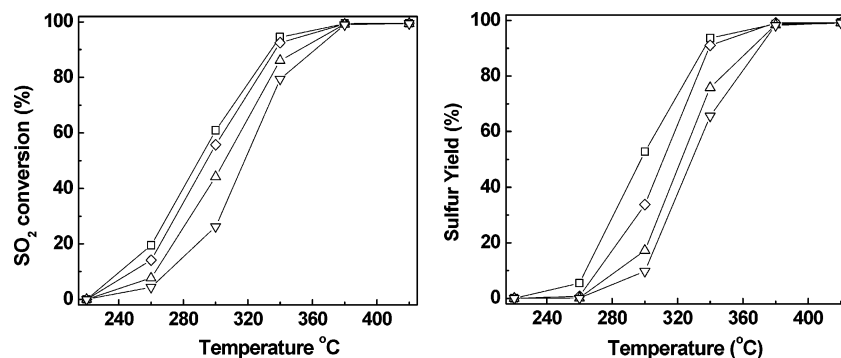


Figure 12. Effect of feed concentration (CO: SO_2 , ppm) on SO_2 conversion and sulfur yield over $\text{Fe}_2\text{O}_3/\gamma\text{-Al}_2\text{O}_3$. (\square) 5000:2500, (\diamond) 10 000:5000, (Δ) 15 000:7500, and (∇) 20 000:10 000.

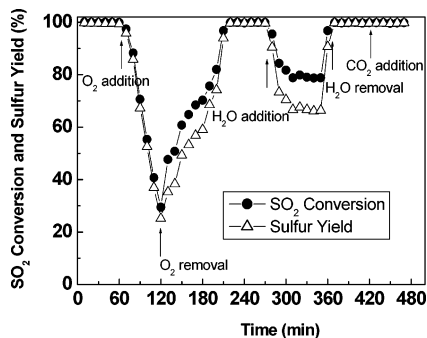


Figure 13. Effect of O_2 , H_2O , or CO_2 addition on SO_2 conversion and sulfur yield over $\text{Fe}_2\text{O}_3/\gamma\text{-Al}_2\text{O}_3$ at 400 °C. Feed compositions: 5000 ppm SO_2 , 10 000 ppm CO, 0.5% O_2 or 4% H_2O or 10% CO_2 , SV = 18 000 mL/g h.

99.83% to 79.01% and was maintained unchanged. It was also found that the SO_2 conversion could be recovered in a very short time when the water vapor was removed from the feed gas. Ma et al.²⁸ reported a similar result over the lanthanum

oxysulfide catalyst. In contrast, when 10% CO_2 was added to the feed gas, no decay in catalytic activity was found.

3.5. Stability of the $\text{Fe}_2\text{O}_3/\gamma\text{-Al}_2\text{O}_3$. The time dependence of the CO– SO_2 reaction over presulfided 20% $\text{Fe}_2\text{O}_3/\gamma\text{-Al}_2\text{O}_3$ was investigated at 380 °C and 400 °C, respectively. As illustrated in Figure 14, the conversion of SO_2 and the sulfur yield dropped only about 2% after a 30 h run at 380 °C, while no deactivation was observed at 400 °C, showing a good stability of the $\text{Fe}_2\text{O}_3/\gamma\text{-Al}_2\text{O}_3$.

3.6. Comparison with Other Catalysts. According to the literature, $\text{CoMo}/\gamma\text{-Al}_2\text{O}_3$ ¹⁹ and $\text{Cr}_2\text{O}_3/\text{nano-CeO}_2$ ¹⁴ were the most active catalysts reported so far for SO_2 reduction with CO. However, the high cost of nano- CeO_2 greatly limits its application on a large scale. As for $\text{CoMo}/\gamma\text{-Al}_2\text{O}_3$, complete conversion of SO_2 was achieved at 300 °C, which was lower than that over the $\text{Fe}_2\text{O}_3/\gamma\text{-Al}_2\text{O}_3$ catalyst we employed in the present work. But the different textural properties of $\gamma\text{-Al}_2\text{O}_3$, especially the surface area, would have a great influence on the catalytic activity. The surface area of the $\gamma\text{-Al}_2\text{O}_3$ used in $\text{CoMo}/\gamma\text{-Al}_2\text{O}_3$ was 333 m^2/g ,¹⁹ while it is only 238 m^2/g in our $\text{Fe}_2\text{O}_3/\gamma\text{-Al}_2\text{O}_3$.

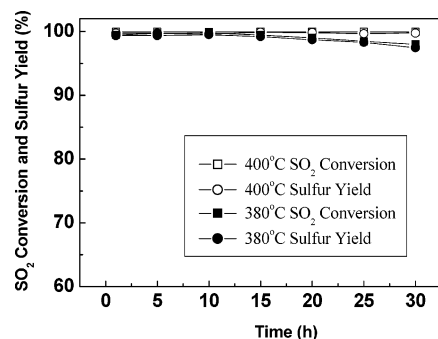


Figure 14. Stability of $\text{Fe}_2\text{O}_3/\gamma\text{-Al}_2\text{O}_3$ catalyst under 380 °C and 400 °C. Feed compositions: 5000 ppm SO_2 and 10000 ppm CO, SV = 18 000 mL/g h.

Moreover, our latest results show that a full SO_2 conversion can be obtained at 300 °C when the high-surface-area $\gamma\text{-Al}_2\text{O}_3$ (448 m^2/g) is used. Therefore, we believe that $\text{Fe}_2\text{O}_3/\gamma\text{-Al}_2\text{O}_3$ is one of best catalysts for the catalytic reduction of SO_2 to sulfur with CO.

4. Conclusions

Among the four different supported iron oxide catalysts, both $\text{Fe}_2\text{O}_3/\gamma\text{-Al}_2\text{O}_3$ and $\text{Fe}_2\text{O}_3/\text{ZSM-5}$ exhibited good performance for the reduction of sulfur dioxide by carbon monoxide. Presulfidation is necessary and important. FeS_2 is the key active phase for this reaction, and its formation depends not only on the acidic nature of the support but also on the presulfidation conditions employed. In addition, the acidity of the support can speed up the reaction between COS and SO_2 . Under the optimal conditions, that is, an Fe content of 20 wt %, presulfidation at 500 °C for 2 h, and a CO/ SO_2 ratio of 2:1, a 99.31% SO_2 conversion and a 99.17% sulfur yield were obtained at 380 °C over $\text{Fe}_2\text{O}_3/\gamma\text{-Al}_2\text{O}_3$.

Acknowledgment

Financial support from the National Science Foundation of China for Distinguished Young Scholars (20325620) is gratefully acknowledged.

Literature Cited

- (1) Flytzani-Stephanopoulos, M.; Zhu, T.; Li, Y. Ceria-based catalysts for the recovery of elemental sulfur from SO_2 -laden gas streams. *Catal. Today* **2000**, *62*, 145.
- (2) Yu, J. J.; Yu, Q.; Jin, Y.; Chang, S. G. Reduction of sulfur dioxide by methane to elemental sulfur over supported cobalt catalysts. *Ind. Eng. Chem. Res.* **1997**, *36*, 2128.
- (3) Jin, Y.; Yu, Q.; Chang, S. G. Reduction of sulfur dioxide by syngas to elemental sulfur over iron-based mixed oxide supported catalyst. *Environ. Prog.* **1997**, *16*, 1.
- (4) Zhu, T.; Kundakovic, L.; Dreher, A.; Flytzani-Stephanopoulos, M. Redox chemistry over CeO_2 -based catalysts: SO_2 reduction by CO or CH_4 . *Catal. Today* **1999**, *50*, 381.
- (5) Lepsoe, R. Chemistry of Sulfur Dioxide Reduction. *Ind. Eng. Chem.* **1938**, *30*, 92.
- (6) Lepsoe, R. Chemistry of Sulfur Dioxide Reduction Kinetics. *Ind. Eng. Chem.* **1940**, *32*, 910.
- (7) Happel, J.; Hnatow, M. A.; Bajars, L.; Kundrath, M. Lanthanum Titanate catalyst—sulfur dioxide reduction. *Ind. Eng. Chem. Prod. Res. Dev.* **1975**, *14*, 154.

- (8) Baglio, J. A. Lanthanum oxysulfide as a catalysts for the oxidation of CO and COS by SO_2 . *Ind. Eng. Chem. Prod. Res. Dev.* **1982**, *21*, 38.
- (9) Hibbert, D. B.; Campbell, R. H. Flue gas desulphurisation: Catalytic removal of sulfur dioxide by carbon monoxide on sulphided $\text{Sr}_x\text{La}_{1-x}\text{CoO}_3$: I. Adsorption of sulphur dioxide, carbon monoxide and their mixtures. *Appl. Catal.* **1988**, *41*, 273.
- (10) Hibbert, D. B.; Campbell, R. H. Flue gas desulphurisation: Catalytic removal of sulfur dioxide by carbon monoxide on sulphided $\text{Sr}_x\text{La}_{1-x}\text{CoO}_3$: II. Reaction of sulphur dioxide and carbon monoxide in a flow system. *Appl. Catal.* **1988**, *41*, 289.
- (11) Liu, W.; Sarofim, A. F.; Flytzani-Stephanopoulos, M. Reduction of sulfur dioxide by carbon monoxide to elemental sulfur over composite oxide catalysts. *Appl. Catal., B* **1994**, *4*, 167.
- (12) Ma, J.; Fang, M.; Lau, N. T. On the synergism between $\text{La}_2\text{O}_3\text{-CoS}_2$ in the reduction of SO_2 to elemental sulfur by CO. *J. Catal.* **1996**, *158*, 251.
- (13) Ma, J.; Fang, M.; Lau, N. T. Activation of La_2O_3 for the catalytic reduction of SO_2 by CO. *J. Catal.* **1996**, *163*, 271.
- (14) Chen, C. L.; Weng, H. S. Nanosized CeO_2 -supported metal oxide catalysts for catalytic reduction of SO_2 with CO as a reducing agent. *Appl. Catal., B* **2004**, *55*, 109.
- (15) Kim, H.; Park, D. W.; Woo, H. C.; Chung, J. S. Reduction of SO_2 by CO to elemental sulfur over $\text{Co}_3\text{O}_4\text{-TiO}_2$ catalysts. *Appl. Catal., B* **1998**, *10*, 233.
- (16) Khallafalla, S. E.; Foerster, E. F.; Hass, L. A. Catalytic reduction of sulfur dioxide on iron-alumina bifunctional catalysts. *Ind. Eng. Chem. Prod. Res. Dev.* **1971**, *10*, 133.
- (17) Khallafalla, S. E.; Hass, L. A. The role of metallic component in the iron-alumina bifunctional catalyst for reduction of SO_2 with CO. *J. Catal.* **1972**, *24*, 121.
- (18) Goetz, V. N.; Sood, A.; Kittrell, J. R. Catalyst evaluation for the simultaneous reduction of sulfur dioxide and nitric oxide by carbon monoxide. *Ind. Eng. Chem. Prod. Res. Dev.* **1974**, *13*, 110.
- (19) Zhuang, S. X.; Magara, H.; Yamazaki, M.; Takahashi, Y.; Yamada, M. Catalytic conversion of CO, NO and SO_2 on the supported sulfide catalyst: I. Catalytic reduction of SO_2 by CO. *Appl. Catal., B* **2000**, *24*, 89.
- (20) Lee, H. M.; Han, J. D. Catalytic reduction of sulfur dioxide by carbon monoxide over nickel and lanthanum—nickel supported on alumina. *Ind. Eng. Chem. Res.* **2002**, *41*, 2623.
- (21) Hass, L. A.; Khalafalla, S. E. Kinetic evidence of a reactive intermediate in reduction of SO_2 with CO. *J. Catal.* **1973**, *29*, 264.
- (22) Inui, T.; Pu, S. B.; Kugai, J. I. Selective neutralization of acid sites on the external surface of HZSM-5 crystallites by a mechanochemical method for methylation of methylanthralene. *Appl. Catal., A* **1996**, *146*, 285.
- (23) Corma, A.; Fornes, V.; Juan-Rafadell, M. I. Influence of preparation conditions on the structure and catalytic properties of $\text{SO}_4^{2-}/\text{ZrO}_2$ superacid catalysts. *Appl. Catal., A* **1994**, *116*, 151.
- (24) Wang, Y.; Chen, Q.; Yang, W.; Xie, Z.; Xu, W.; Huang, D. Effect of support nature on WO_3/SiO_2 structure and butene-1 metathesis. *Appl. Catal., A* **2003**, *250*, 25.
- (25) Diez, V. K.; Apesteguia, C. R.; Di Cosium, J. I. Acid-base properties and active site requirements for elimination reactions on alkali-promoted MgO catalysts. *Catal. Today* **2000**, *63*, 53.
- (26) Munteanu, G.; Ilieva, L.; Andreeva, D. Kinetic parameters obtained from TPR data for $\alpha\text{-Fe}_2\text{O}_3$ and $\text{Au}/\alpha\text{-Fe}_2\text{O}_3$ systems. *Thermochim. Acta* **1997**, *291*, 171.
- (27) Lobree, L. J.; Hwang, I. C.; Reimer, J. A.; Bell, A. T. Investigations of the state of Fe in H-ZSM-5. *J. Catal.* **1999**, *186*, 242.
- (28) Ma, J.; Fang, M.; Lau, N. T. The catalytic reduction of SO_2 by CO over lanthanum oxysulphide. *Appl. Catal., A* **1997**, *253*, 268.

Received for review January 20, 2006

Revised manuscript received March 23, 2006

Accepted April 28, 2006